JOURNAL OF COMPUTATIONAL PHYSICS 21, 438–453 (1976)

A Numerical Technique for Low-Speed Homogeneous Two-Phase Flow with Sharp Interfaces*

JOHN D. RAMSHAW† AND JOHN A. TRAPP

Aerojet Nuclear Company, 550 Second Street, Idaho Falls, Idaho 83401

Received December 18, 1975

A numerical method is presented for calculating the transient flow of a homogeneous two-phase (gas–liquid) fluid at small Mach numbers. The method is Eulerian and is applicable in one, two, or three space dimensions. The density ratio of the two phases may be arbitrarily large, enabling the important special case of steam–water flow at low pressures to be treated. The phase interface is resolved by using a modified donor–acceptor differencing technique for computing mass transport. Inaccuracies resulting from slightly inconsistent calculations of mass and energy transport are avoided by converting the energy equation into a form which does not involve a convective derivative. A nonconservative form of the momentum equation is utilized because velocity is typically a smoother function than momentum density when the phase density ratio is large. The results of two sample calculations are presented.

1. INTRODUCTION

A number of problems of practical importance involve the low-speed flow of a single-component two-phase fluid with a large phase density ratio and a moving phase interface. In nuclear reactor safety analysis, for example, such problems arise in connection with (a) the reflooding of a steam-filled reactor core following a loss-of-coolant accident by liquid water from the emergency core cooling system, and (b) the venting of steam into a liquid water suppression pool having a free surface. This paper presents a new numerical technique for solving problems of this general type.

The numerical solution of such problems is hindered by the fact that the field variables do not vary slowly in comparison with practical finite-difference mesh spacings—enormous gradients of density and internal energy occur at the phase interface. In general, even moderately large gradients are known to lead to inaccurate results in Eulerian fluid flow calculations because of excessive numerical

* Work performed under Energy Research and Development Administration (ERDA) Contract AT(10-1)-1375.

† Now with Los Alamos Scientific Laboratory, P.O. Box 1663, Los Alamos, N.M. 87545.

diffusion or smearing [1, 2]. In addition, large density and energy gradients, in combination with slight numerical discrepancies between the mass and energy transport calculations, can cause unacceptable errors in the calculated pressure and velocity [3]. In the present context, the gradients are so extremely large that special care must be taken to avoid these problems. The numerical technique described in this paper has been specifically designed to eliminate these particular sources of error, and still retain the simplicity of a basically Eulerian formulation.

A number of methods have been described for the numerical treatment of fluid interfaces; Ref. [4] and references cited therein discuss a number of these methods. Most of these methods are somewhat complicated and cumbersome to implement, and are not directly applicable to single-component two-phase interface problems, in which mass exchange between phases may spontaneously occur during the flow process. The method we have adopted to represent the phase interface without numerical smearing is to compute mass transport by a modified donor–acceptor (DA) differencing procedure [5, 6]. The DA technique was chosen for two reasons: (1) It is easy to incorporate into the framework of an Eulerian computing method; and (2) it is easy to adapt to the single-component two-phase case, and requires no explicit modification to allow for phase transitions. The disadvantage of the DA technique is that, unlike the other interface techniques, it does not resolve the interface in detail within a computational cell. For this reason it is not very suitable for calculating physical effects (such as surface-wave instability) whose accurate representation requires a detailed knowledge of the interface configuration. This limitation can in principle be overcome (except for surface tension effects) by using very fine zoning.

The use of donor–acceptor differencing to prevent interface smearing is an essential feature of our method. Another essential feature is the conversion of the energy equation into a form which does not involve a convective derivative. This approach appears to be novel; it has the advantage of eliminating any possibility of numerical inconsistencies between the mass and energy transport calculations. The pressure and velocity errors which might otherwise arise from this source are thus rigorously prohibited.

Another somewhat unusual feature of our method is the use of a nonconservative difference analog of the momentum equation. This procedure was adopted because in problems of present interest the velocity $\mathbf{u}$ varies much more slowly in space and time than does the momentum density $\rho\mathbf{u}$. Overall accuracy is thereby enhanced considerably, in spite of the loss of rigorous momentum conservation.

Because of the manner in which the momentum and energy equations are treated, donor–acceptor differencing is needed and used only in the continuity equation.

The remainder of our numerical technique is more or less conventional, and is closely related to the Chorin–Hirt modification of the MAC method for incom-

pressible flow [7]. The pressure gradient in the momentum equation, the velocity in the continuity equation, and the velocity divergence in the energy equation are treated implicitly. The remaining terms in the equations are treated explicitly. The implicit part of the scheme is solved by an iterative procedure very similar to that of Hirt and Cook [7]. A detailed description of the method is given in the subsequent discussion and is followed by two sample calculations.

2. The Basic Equations

The basic equations for the transient flow of a single-component homogeneous two-phase (gas–liquid) fluid are

$$D\rho/Dt = -\rho\nabla \cdot \mathbf{u}, \tag{1}$$

$$\rho(D\mathbf{u}/Dt) = -\nabla p + \nabla \cdot \boldsymbol{\tau} + \rho\mathbf{g}, \tag{2}$$

$$\rho(DI/Dt) = -p\nabla \cdot \mathbf{u} + \boldsymbol{\tau} : \nabla\mathbf{u} - \nabla \cdot \mathbf{J}, \tag{3}$$

$$\rho = f(p, I), \tag{4}$$

where ρ is the mass density, $\mathbf{u}$ the velocity, p the pressure, $\boldsymbol{\tau}$ the viscous (deviatoric) stress tensor, $\mathbf{g}$ the acceleration of gravity, I the specific internal energy, and $\mathbf{J}$ the heat flux vector. The symbol D/Dt represents the convective derivative $\partial/\partial t + \mathbf{u} \cdot \nabla$. Equations (1) through (4) must of course be supplemented by constitutive equations for $\boldsymbol{\tau}$ and $\mathbf{J}$, normally the Newtonian Law for $\boldsymbol{\tau}$ and the Fourier Law for $\mathbf{J}$.

The state relation, Eq. (4), applies in both the single-phase and the two-phase regions. The derivatives $(\partial\rho/\partial I)_p$ and $(\partial\rho/\partial p)_I$ are discontinuous at the boundary between these regions. Several auxiliary state variables and relationships exist. For any pressure p less than the critical pressure, the liquid and gas saturation densities $\rho_l(p)$ and $\rho_g(p)$ are well defined. The quality x and void fraction α are then defined in terms of the saturation densities by the relations

$$\begin{aligned} \alpha &= 0 && \text{if } \rho \geqslant \rho_l, \\ &= (\rho - \rho_l)/(\rho_g - \rho_l) && \text{if } \rho_g < \rho < \rho_l, \\ &= 1 && \text{if } \rho \leqslant \rho_g, \end{aligned} \tag{5}$$

$$x = [1 + (\rho_l/\rho_g)((1/\alpha) - 1)]^{-1}. \tag{6}$$

The local mass fraction of the gas phase is x, and the local volume fraction is α.

We now wish to express the energy equation, Eq. (3), in an alternative form which will be convenient for numerical solution by finite-difference methods. By

substituting Eq. (4) into Eq. (1) and using Eq. (3) to eliminate DI/Dt, the following net result is obtained:

$$(\nabla \cdot \mathbf{u})\left[p\left(\frac{\partial \rho}{\partial I}\right)_p - \rho^2\right] = \left(\frac{\partial \rho}{\partial I}\right)_p (\boldsymbol{\tau} : \nabla \mathbf{u} - \nabla \cdot \mathbf{J}) + \rho\left(\frac{\partial \rho}{\partial p}\right)_I \frac{Dp}{Dt}. \tag{7}$$

Equation (7) is really a combination of the energy, continuity, and state equations. In this paper it is regarded as an equivalent form of the energy equation because it is used to replace Eq. (3) while Eqs. (1) and (4) are retained.

At this point attention is explicitly restricted to the case of small Mach number. This case may be realized by assuming the isentropic sound speed $C = (\partial p/\partial \rho)_s^{1/2}$ to be very large. This assumption, together with the thermodynamic relation

$$\rho(\partial \rho/\partial p)_I[p(\partial \rho/\partial I)_p - \rho^2]^{-1} = -1/(\rho C^2), \tag{8}$$

implies that the last term in Eq. (7) becomes negligibly small and can be omitted. Equation (7) then reduces to

$$\nabla \cdot \mathbf{u} = [p - \rho^2(\partial I/\partial \rho)_p]^{-1} (\boldsymbol{\tau} : \nabla \mathbf{u} - \nabla \cdot \mathbf{J}), \tag{9}$$

which may be regarded as an incompressibility condition.

When ρ is independent of I (or, alternatively, in the absence of viscosity and heat conduction), Eq. (9) reduces to $\nabla \cdot \mathbf{u} = 0$, the usual incompressibility condition for the case in which ρ is constant for a given fluid particle. Equation (9) is the generalization of this condition to allow for local thermal expansion or contraction. This interpretation becomes intuitively clear when it is noted that $\boldsymbol{\tau} : \nabla \mathbf{u} - \nabla \cdot \mathbf{J}$ is the local volumetric rate of energy buildup, and that

$$p - \rho^2(\partial I/\partial \rho)_p = (\partial h/\partial v)_p, \tag{10}$$

where h is the specific enthalpy and $v = 1/\rho$ is the specific volume.

The basic equations for the transient flow of a single-component homogeneous two-phase fluid at small Mach number may now be taken to be Eqs. (1), (2), (4), and (9). The restriction to small Mach numbers implies that the local fluid velocity must be small relative to the sound speed in both phases for these equations to be applicable.

3. The Numerical Scheme

The numerical solution of Eqs. (1), (2), (4), and (9) is effected by constructing finite-difference analogs of them; the resulting finite-difference equations are then programmed for solution by a high-speed digital computer. It is convenient for

clarity to begin by exhibiting the temporal differencing of Eqs. (1), (2), (4), and (9) explicitly while suppressing the spatial differencing:

$$\rho^n \left(\frac{\mathbf{u}^{n+1} - \mathbf{u}^n}{\Delta t} + \mathbf{u}^n \cdot \nabla \mathbf{u}^n \right) = -\nabla p^{n+1} + \nabla \cdot \tau^n + \rho^n \mathbf{g}, \tag{11}$$

$$\nabla \cdot \mathbf{u}^{n+1} = \frac{\tau^n : \nabla \mathbf{u}^n - \nabla \cdot \mathbf{J}^n}{p^n - (\rho^n)^2 (\partial I / \partial \rho)_p^n}, \tag{12}$$

$$\frac{\rho^{n+1} - \rho^n}{\Delta t} + \nabla \cdot (\rho^n \mathbf{u}^{n+1}) = 0, \tag{13}$$

$$\rho^{n+1} = f(p^{n+1}, I^{n+1}), \tag{14}$$

where Δt is the time increment and A^n denotes the difference analog of the quantity A at time $n\Delta t$. All spatial derivatives in Eqs. (11) through (13) are to be replaced by spatial differences in a manner to be described presently. The sequence of a calculational cycle is as follows. Equations (11) and (12) are first solved simultaneously, by an iterative procedure, to obtain p^{n+1} and $\mathbf{u}^{n+1}$. Equation (13) is then solved for ρ^{n+1}. Finally, I^{n+1} is obtained by inversion of Eq. (14).

With the exception of the convective term $\nabla \cdot (\rho^n \mathbf{u}^{n+1})$ in Eq. (13), which is differenced according to a modified donor–acceptor rule, the spatial differencing of Eqs. (11) through (13) is closely patterned after that of [7], a paper with which the reader is assumed to be familiar. The region of computation is divided into small finite-difference cells of dimensions Δx, Δy, and Δz and labeled by integer indices (i, j, k). The thermodynamic variables p, ρ, and I are defined at cell centers whereas the velocity components (u, v, w) are defined at cell faces.

Except for two minor differences, the spatial differencing of Eq. (11) is identical to that of the corresponding equation in [7], and hence will not be displayed in detail. The first difference is that the density is not constant in the present context; the densities in Eq. (11) are evaluated at the cell face on which the velocity component in question is defined, by averaging the adjacent cell-centered densities. For example, in the calculation of $v_{i,j+1/2,k}^{n+1}$ the density ρ^n in Eq. (11) is evaluated as

$$\tfrac{1}{2}(\rho_{i,j,k}^n + \rho_{i,j+1,k}^n) \equiv \rho_{i,j+1/2,k}^n .$$

The second difference is that, unlike Hirt and Cook, we do not limit ourselves to centered space differencing of the convective terms in Eq. (11). Instead, a weighted average between centered and donor-cell differencing [3, 8] is allowed. The weighting factor may be chosen to nullify a destabilizing truncation error [3, 9] so that viscosity is no longer required for numerical stability.

Equation (12) is evidently a cell-centered equation; all terms in it are evaluated

at cell centers, the spatial derivatives being represented by simple centered differences. For example,

$$[\nabla \cdot \mathbf{u}^{n+1}]_{ijk} = \frac{1}{\Delta x}(u^{n+1}_{i+1/2,j,k} - u^{n+1}_{i-1/2,j,k}) + \frac{1}{\Delta y}(v^{n+1}_{i,j+1/2,k} - v^{n+1}_{i,j-1/2,k}) + \frac{1}{\Delta z}(w^{n+1}_{i,j,k+1/2} - w^{n+1}_{i,j,k-1/2}), \tag{15}$$

where the notation $[A]_{ijk}$ represents the spatial difference approximation to the quantity A at the center of cell (i, j, k).

The iterative procedure by which the simultaneous solution of Eqs. (11) and (12) is effected is essentially identical to that of Hirt and Cook. At the beginning of the iteration an explicit advancement of the velocity components is performed, which serves to evaluate the terms at time level n in Eq. (11). The iteration then proceeds by simultaneous adjustments of pressure and the velocity components to make the velocity divergence satisfy Eq. (12). The pressure change in a given cell over one iteration is given by

$$\delta p_{ijk} = -\beta(D_{ijk} - S^n_{ijk}), \tag{16}$$

where D_{ijk} is the current value of the velocity divergence and S^n_{ijk} denotes the spatially differenced form of the right-hand side of Eq. (12). As recommended by Viecelli [10], D_{ijk} is evaluated using all available new velocity iterates to accelerate convergence. The weighting factor β is given by

$$\beta = \frac{\beta_0}{\Delta t}\left[\frac{1}{\Delta x^2}\left(\frac{1}{\rho^n_{i+1/2,j,k}} + \frac{1}{\rho^n_{i-1/2,j,k}}\right) + \frac{1}{\Delta y^2}\left(\frac{1}{\rho^n_{i,j+1/2,k}} + \frac{1}{\rho^n_{i,j-1/2,k}}\right) + \frac{1}{\Delta z^2}\left(\frac{1}{\rho^n_{i,j,k+1/2}} + \frac{1}{\rho^n_{i,j,k-1/2}}\right)\right]^{-1}, \tag{17}$$

where $0 < \beta_0 < 2$ for iteration convergence. With this weighting factor the iteration scheme becomes equivalent to the successive over-relaxation method as applied to the associated Poisson-like pressure equation. The velocity components are changed in correspondence to each pressure change, as required by the momentum equation. The iteration is terminated when the largest value of $|\delta p_{ijk}|$ in the mesh falls below a specified cutoff value, typically 10^{-5} to 10^{-6} of the maximum pressure in the problem. Boundary conditions are reset after every iteration in essentially the same manner as described by Hirt and Cook.

After the iteration has converged, $\mathbf{u}^{n+1}$ is known and Eq. (13) can be solved

explicitly for ρ_{ijk}^{n+1}. The term $\nabla \cdot (\rho^n \mathbf{u}^{n+1})$ in Eq. (13) is spatially differenced by writing it in terms of mass fluxes across cell faces:

$$\begin{aligned}[\nabla \cdot (\rho^n \mathbf{u}^{n+1})]_{ijk} = &\frac{1}{\Delta x}(\hat{\rho}^n_{i+1/2,j,k} u^{n+1}_{i+1/2,j,k} - \hat{\rho}^n_{i-1/2,j,k} u^{n+1}_{i-1/2,j,k}) \\ &+ \frac{1}{\Delta y}(\hat{\rho}^n_{i,j+1/2,k} v^{n+1}_{i,j+1/2,k} - \hat{\rho}^n_{i,j-1/2,k} v^{n+1}_{i,j-1/2,k}) \\ &+ \frac{1}{\Delta z}(\hat{\rho}^n_{i,j,k+1/2} w^{n+1}_{i,j,k+1/2} - \hat{\rho}^n_{i,j,k-1/2} w^{n+1}_{i,j,k-1/2}),\end{aligned} \tag{18}$$

where the face-centered densities $\hat{\rho}$ represent the density of mass actually being transported across the cell face in question. This prescription for mass transport is conservative regardless of how the $\hat{\rho}$ are defined. We choose to define the $\hat{\rho}$ by a modified donor–acceptor rule. The guiding principle of donor–acceptor differencing may be generally stated as follows: in computing transport of a mixture quantity from a donor cell to an acceptor cell, the single-component or -phase values are determined by the donor cell whereas the composition or proportions are determined by the acceptor cell.

In a single-component two-phase mixture, the mixture density ρ is related to the phase densities ρ_l and ρ_g by

$$\rho = \alpha \rho_g + (1 - \alpha)\, \rho_l\,,$$

which follows from Eq. (5). Thus in dealing with density α can be regarded as determining the composition of the two-phase mixture. Clearly α may be considered as a cell-centered quantity α^n_{ijk}, defined by Eq. (5) with ρ replaced by ρ^n_{ijk} and with ρ_l and ρ_g replaced by $\rho(p^n_{ijk})$ and $\rho_g(p^n_{ijk})$, respectively. With this background, our donor–acceptor prescription for ρ can be mathematically expressed as

$$\begin{aligned}\hat{\rho}^n_{i+1/2,j,k} &= \rho_D{}^n \qquad \text{if } \alpha_D{}^n = 0 \text{ or } \alpha_D{}^n = 1 \text{ or } |\, \alpha_D{}^n - \alpha_A{}^n\,| < 0.001, \\ &= \alpha_A{}^n \rho^n_{gD} + (1 - \alpha_A{}^n)\, \rho^n_{lD} \qquad \text{otherwise,}\end{aligned} \tag{19}$$

where the subscripts D and A, which denote the donor and acceptor cells, are defined by

$$\begin{aligned} &D = (i, j, k) \\ &A = (i + 1, j, k) \end{aligned} \Bigg\} \quad \text{if } u^{n+1}_{i+1/2,j,k} > 0, \tag{20}$$

$$\begin{aligned} &D = (i + 1, j, k) \\ &A = (i, j, k) \end{aligned} \Bigg\} \quad \text{if } u^{n+1}_{i+1/2,j,k} < 0.$$

The densities $\hat{\rho}^n_{i,j+1/2,k}$ and $\hat{\rho}^n_{i,j,k+1/2}$ are of course defined by similar expressions.

The preceding prescription is a physically reasonable way to prevent interface smearing. For example, if D is a two-phase cell and A is a pure gas cell then $\alpha_A{}^n = 1$ and $\hat{\rho}^n = \rho_{gD}^n$. That is, pure gas is transported into a pure gas cell from a two-phase cell until all the gas in the two-phase cell is exhausted.

The condition on $| \alpha_D{}^n - \alpha_A{}^n |$ in Eq. (19) is a cutoff constraint which causes the transport between two adjacent cells of nearly the same composition to be computed by a pure donor-cell procedure even when the donor cell D is in the two-phase region. Failure to include such a cutoff can result in the spontaneous development of large density gradients in two-phase regions where the liquid and gas phases are well mixed and would be expected to remain so, but where persistent gradients in p (and hence in ρ_l and ρ_g) exist.

One further constraint must be added to the mass transport logic outlined above. The case in which D is a two-phase cell and A is a pure gas cell is again considered, but with $\alpha_D{}^n$ assumed to be much smaller than $| u | \Delta t/\Delta x$. In this case the donor–acceptor prescription as described would transport more gas out of D than D in fact contained; the net effect would be to leave too much liquid mass in D. In this way the cell D would become "overfilled" with liquid and would be forced unphysically to move into the subcooled region ($\rho > \rho_l$). Similarly, if A is a pure liquid cell and $1 - \alpha_D{}^n \ll | u | \Delta t/\Delta x$, the donor–acceptor prescription would transport too much liquid out of D, leaving it with an unphysically small (perhaps even negative) density. In order to avoid these problems, the density of a cell is not allowed to change from a two-phase value to a subcooled or superheated value during a single timestep. When such a change would otherwise occur, the density in question is set equal to the saturation value. The resulting change in mass is compensated by an equal but opposite change in a neighboring cell, so that overall mass conservation is maintained. Because of the inherent lack of resolution in donor–acceptor interface differencing, the choice of the appropriate neighboring cell is not critical.

The spatial differencing of Eq. (14) is trivial; all quantities are cell-centered and simply require the addition of subscripts *ijk*.

Numerical stability and accuracy restrictions are essentially the same as those reported by Hirt and Cook [7], except that the lower limits on viscosity are alleviated by the use of partial donor-cell differencing in the momentum flux terms, as discussed above.

The difference equations described have been programmed for solution in a developmental computer code. The functional relations $\rho = f(p, I)$, $\rho_l(p)$, and $\rho_g(p)$ are evaluated numerically by a table lookup and interpolation procedure developed by R. J. Wagner [11], which represents the thermodynamic properties of water–steam as given by the 1967 IFC Formulation [12, 13]. The code can be applied to problems in one, two, or three dimensions in Cartesian coordinates. The results of two sample calculations are presented in the next section.

4. Sample Calculations

A simple but quite stringent test problem for the numerical technique described in the preceding section is that of calculating one-dimensional oscillations in water level in a vertical pipe of length L subject to a constant pressure drop Δp, in the absence of viscosity and thermal conductivity. The velocity is uniform along the length of the pipe by virtue of Eq. (9), and hence is a function of time alone. Initially the pipe is filled with water of density ρ_l to a height H_0, and with steam of density ρ_g above H_0; the initial velocity is u_0. By writing a force balance on the material within the pipe, we find that the motion is governed by the following ordinary differential equation for the water height $H(t)$:

$$\frac{d^2H}{dt^2} = \frac{\Delta p}{\rho_l H + \rho_g(L - H)} - g, \tag{21}$$

subject to the initial conditions $H = H_0$ and $dH/dt = u_0$ at $t = 0$. This equation has been solved numerically, by a standard method, for the following values of the parameters:

$$L = 3.6576 \text{ m}, \qquad H_0 = 1.09728 \text{ m},$$
$$u_0 = 0.0 \text{ m/sec}, \qquad \Delta p = 1.757 \times 10^4 \text{ N/m}^2,$$
$$\rho_l = 920.048 \text{ kg/m}^3, \qquad \rho_g = 2.2325 \text{ kg/m}^3.$$
$$g = 9.8 \text{ m/sec}^2,$$

(These density values are very close to the saturation values at $p = 4.137$ bar.) The resulting time dependence of $u = dH/dt$ is shown as the solid curve in Fig. 1, which

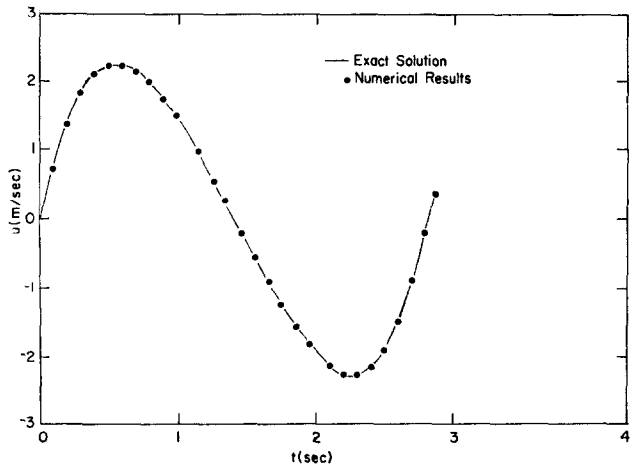

Fig. 1. Velocity oscillations in vertical pipe under constant pressure drop.

may be regarded as the exact solution. The problem is seen to exhibit oscillatory behavior in velocity and hence in water level.

The same problem was run with the numerical scheme described in Section 3, at an ambient pressure of 4.137 bar, using 20 spatial cells ($\Delta x = 0.18288$ m) and a timestep of $\Delta t = 0.005$ sec. The resulting velocity curve is shown by the circular points on Fig. 1; the agreement with the exact solution is seen to be excellent. The velocities were not quite uniform along the pipe because of the finite iteration convergence criterion (for this problem, the cutoff was $| \delta p |/p_{\max} = 5 \times 10^{-6}$), but were generally uniform to within 0.5% or better. Figure 2 is a logarithmic plot of

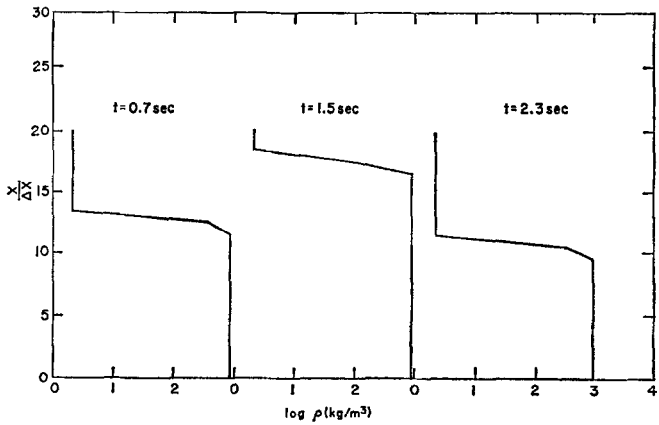

FIG. 2. Logarithmic density profiles at $t = 0.7$, 1.5, and 2.3 sec.

the density profiles (unsmoothed) at three different times during the calculation. These plots show that the calculation preserved the sharp water–steam interface without appreciable smearing, even though the density ratio is almost 1000:1.

The second test calculation is that of liquid water sloshing in a two-dimensional rectangular tank of length L and height H. The tank is half-filled with liquid water and half-filled with steam. The initial conditions are: (1) All the liquid water is in the right-hand side of the tank, (2) the pressure is uniform at the value p_0, and (3) the velocity is zero. The calculation was run with the parameter values

$$\begin{aligned} L &= 1.0 \text{ m}, & H &= 0.5 \text{ m}, \\ \Delta x &= L/20, & \Delta z &= H/10, \\ \rho_l &= 960.0 \text{ kg/m}^3, & \rho_g &= 0.585 \text{ kg/m}^3, \\ p_0 &= 1.0 \text{ bar}, & \Delta t &= 0.005 \text{ sec}. \end{aligned}$$

Viscosity and heat conduction were neglected, and free slip boundary conditions

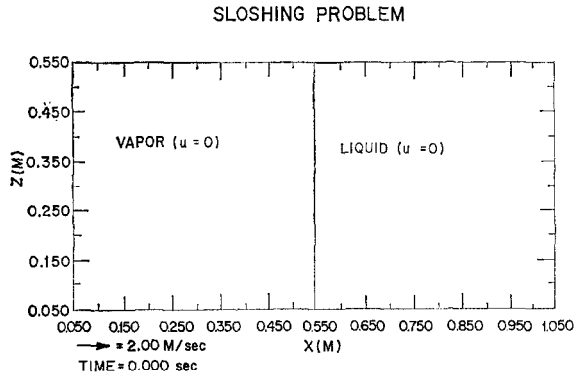

FIG. 3a. Sloshing problem $t = 0.0$ sec.

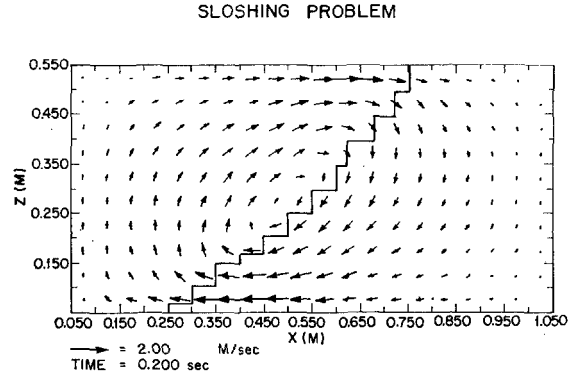

FIG. 3b. Sloshing problem $t = 0.2$ sec.

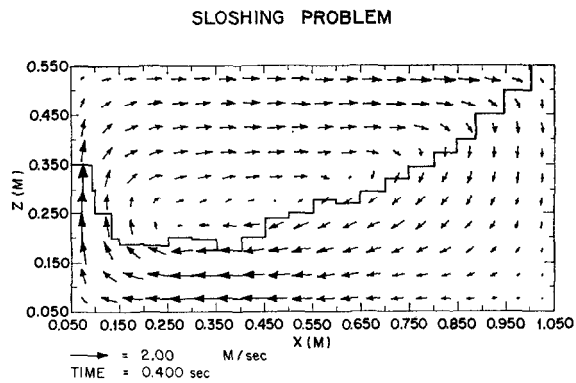

FIG. 3c. Sloshing problem $t = 0.4$ sec.

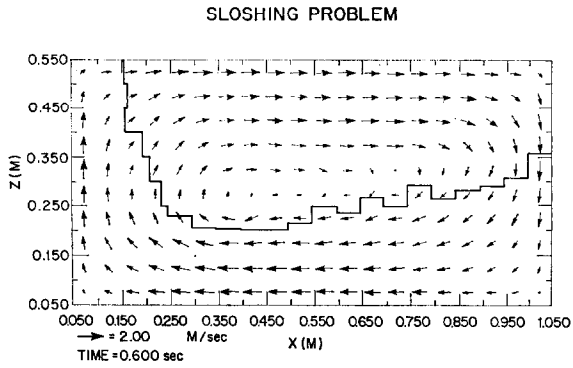

FIG. 3d. Sloshing problem $t = 0.6$ sec.

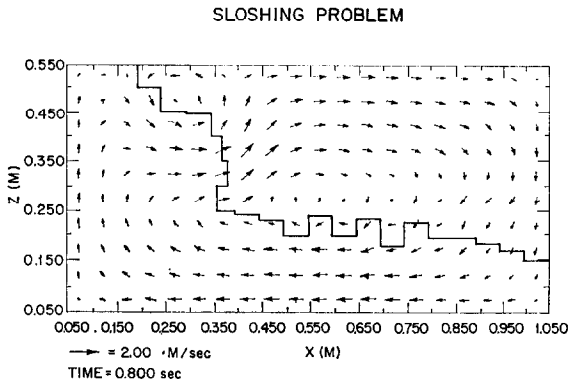

FIG. 3e. Sloshing problem $t = 0.8$ sec.

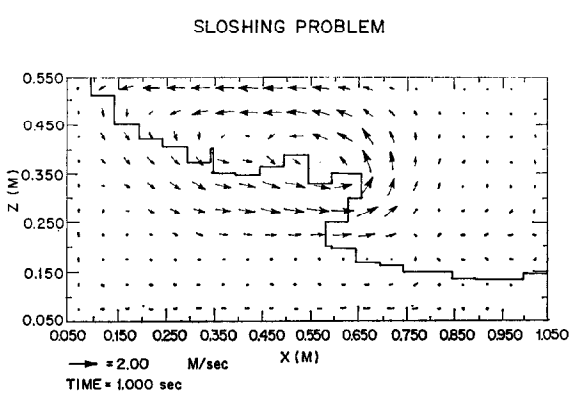

FIG. 3f. Sloshing problem $t = 1.0$ sec.

were imposed. Thus, if no numerical damping were to occur, the sloshing would go on forever.

The development of the motion out to $t = 1.0$ sec is shown in Fig. 3, which shows combined velocity vector plots and interface configuration plots. The interface configuration was plotted by hand from the computer output according to the following procedure. Any cell with $\rho_g < \rho < \rho_l$ is an interface cell. Within each interface cell the interface was represented by a straight line parallel to one of the two coordinate directions. Since the volume fractions of liquid and gas are known [Eq. (5)], this line is constrained to four possible locations. Of these four possibilities the one was chosen which appeared visually to be the most realistic in its relation to neighboring cells. (For example, the liquid in an interface cell was taken to be contiguous with the liquid in neighboring cells whenever possible.) This procedure results in a "staircase" interface pattern, and was adopted here for two reasons: (1) it minimizes subjectivity in the plotting, and (2) it emphasizes the fact that the DA technique does not resolve the interface in detail within a computational cell. Of course, the "staircase" interface plots could legitimately be smoothed further, if desired, by any procedure which preserves the volume fractions of liquid and gas in the interface cells.

No analytical solution is available for this problem, but the numerical results displayed in Fig. 3 clearly show the qualitative sloshing behavior which would be expected intuitively.

The velocity vectors in Figs. 3d through 3f appear to show an incipient instability near the interface. Fortunately, the irregularities do not grow appreciably following their initial appearance, and thus never become large enough to be troublesome. This behavior may reflect the fact that DA differencing is nearly equivalent to calculating mass fluxes by total acceptor differencing at the interface and donor-cell differencing elsewhere, and thus would be expected to be locally unstable at the interface. To show this near equivalence, a problem is considered in which the velocity is parallel to the interface and constant and pressure (and hence ρ_l and ρ_g as well) is constant in space and time. The interface is assumed to be nearly horizontal in cells $I(n)$, $I(n) - 1$, and $I(n) + 1$ at time level n. For this case, it is easily verified that the donor–acceptor differencing prescription reduces to

$$\frac{\rho_i^{n+1} - \rho_i^n}{\Delta t} + u\frac{\rho_{i+1}^n - \rho_i^n}{\Delta x} = 0 \qquad [i = I(n)],$$

where we have assumed that $u > 0$. However, the local instability resulting from the use of acceptor differencing at the interface would be expected to be bounded by the coupling to neighboring cells, where local disturbances are strongly damped by the donor-cell differencing. Thus it is reasonable to expect global stability of the calculation as a whole, as is observed in practice.

The velocity vectors and interface configuration at $t = 2.0$ sec are shown in Fig. 4. Here the noteworthy features are the presence of isolated "drops" and "bubbles" on the order of one cell width in diameter. Although the gross motion continues to be realistic, the DA technique is inherently incapable of correctly representing the motion of single-cell drops or bubbles. The nature of this deficiency

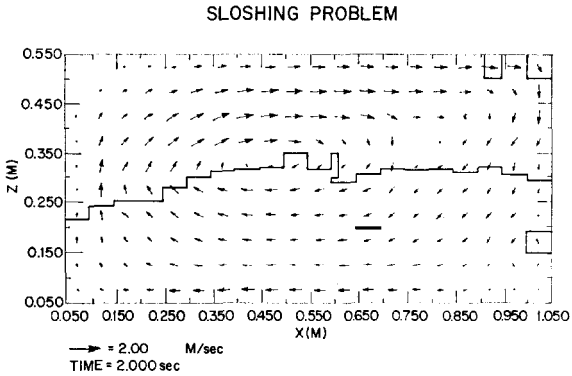

FIG. 4. Sloshing problem $t = 2.0$ sec.

can be seen by considering a one-dimensional problem in which velocity and pressure are constant in space and time. The initial condition is considered to be

$$\begin{aligned} \rho_j^0 &= \alpha_0\rho_g + (1 - \alpha_0)\,\rho_l\,, & j &= J \qquad (0 < \alpha_0 < 1), \\ &= \rho_l\,, & j &\neq J. \end{aligned}$$

Now the value of ρ_j after n timesteps is considered. According to the DA differencing procedure, this value is given by

$$\begin{aligned} \rho_j^n &= \alpha_0\rho_g + (1 - \alpha_0)\,\rho_l\,, & j &= J, \\ &= \rho_l\,, & j &\neq J, \end{aligned} \tag{22}$$

for all n. Physically, however, the bubble should simply translate with velocity u. The correct value for ρ_J^n when $n \geqslant u\,\Delta t/\Delta x$ is, therefore,

$$\rho_J^n = \rho_l\,. \tag{23}$$

From Eq. (22) it is seen that the bubble has remained stationary for all time, instead of moving an additional distance $u\,\Delta t$ as it should have for each time step. This difficulty may be regarded as a result of inadequate finite-difference resolution:

one cannot expect to accurately represent the motion of a drop or bubble with a single cell. If the zoning were refined so that the bubble occupied many cells then the DA technique would again compute essentially correct mass fluxes and hence correct bubble motion.

5. Concluding Remarks

We have described a numerical method for calculating single-component two-phase fluid flow problems at small Mach numbers, while maintaining the integrity of the phase interface. The method may easily be incorporated into the framework of any computer code based on the Chorin–Hirt modification of the MAC method for incompressible flow.

Although we have focused attention on the case of a single-component two-phase fluid, the method described in this paper is equally applicable to problems involving the flow of two different immiscible incompressible fluids separated by a moving interface. Again, no restriction on the density ratio exists. To treat this case, all that is necessary is to replace the zone variables $\rho_l(p^n_{ijk})$ and $\rho_g(p^n_{ijk})$ by constant values ρ_l and ρ_g, to set $(\partial\rho/\partial I)_p = 0$, and to bypass the state routine.

Acknowledgments

We are grateful to C. W. Hirt for calling our attention to the donor–acceptor differencing technique. The three-dimensional computer code which formed the basis for our subsequent modifications was obtained from Science Applications, Inc. (SAI) through a subcontract to Aerojet Nuclear Company. Our initial familiarity with the SAI version of the code was gained largely through helpful discussions with W. J. Wnek. The velocity vector plot routine used in this study was written by G. A. Mortensen. This work was performed under Energy Research and Development Administration (ERDA) Contract AT(10-1)-1375.

References

1. J. E. Welch, F. H. Harlow, J. P. Shannon, and B. J. Daly, "The MAC Method: A Computing Technique for Solving Viscous, Incompressible, Transient Fluid-Flow Problems Involving Free Surfaces," Los Alamos Scientific Laboratory Report LA-3425 (1966).
2. A. A. Amsden, "The Particle-in-Cell Method for the Calculation of the Dynamics of Compressible Fluids," Los Alamos Scientific Laboratory Report LA-3466 (1966).
3. F. H. Harlow and A. A. Amsden, *J. Computational Phys.* **17** (1975), 19.
4. F. H. Harlow and A. A. Amsden, *J. Computational Phys.* **16** (1974), 1.
5. W. E. Johnson, "Development and Application of Computer Programs Related to Hypervelocity Impact," Systems, Science, and Software Report 3SR-353 (1970).

6. J. D. KERSHNER AND C. L. MADER, "2DE: A Two-Dimensional Continuous Eulerian Hydrodynamic Code for Computing Multicomponent Reactive Hydrodynamic Problems," Los Alamos Scientific Laboratory Report LA-4846 (1972).
7. C. W. HIRT AND J. L. COOK, *J. Computational Phys.* **10** (1972), 324.
8. F. H. HARLOW AND A. A. AMSDEN, *J. Computational Phys.* **8** (1971), 197.
9. C. W. HIRT, *J. Computational Phys.* **2** (1968), 339.
10. J. A. VIECELLI, *J. Computational Phys.* **8** (1971), 119.
11. K. V. MOORE AND W. H. RETTIG, "A Computer Program for Transient Thermal-Hydraulic Analysis," Aerojet Nuclear Company Report ANCR-1127 (1973).
12. C. A. MEYER, R. B. MCCLINTOCK, G. J. SILVESTRI, AND R. C. SPENCER, JR., "Thermodynamic and Transport Properties of Steam," American Society of Mechanical Engineers, 1967.
13. E. SCHMIDT, "Properties of Water and Steam in SI Units," Springer–Verlag, New York, 1969.